Preparation of Titania Nanotubes and Their Environmental Applications as Electrode

ARTICLE *in* ENVIRONMENTAL SCIENCE AND TECHNOLOGY · JUNE 2005

Impact Factor: 5.33 · DOI: 10.1021/es048684o · Source: PubMed

4 AUTHORS, INCLUDING:

Shaogui Yang
Nanjing University
96 PUBLICATIONS **1,948** CITATIONS

SEE PROFILE

Environ. Sci. Technol. **2005**, *39,* 3770−3775

Preparation of Titania Nanotubes and Their Environmental Applications as Electrode

XIE QUAN,* SHAOGUI YANG, XIULI RUAN, AND HUIMING ZHAO

School of Environmental and Biological Science and Technology, Dalian University of Technology, Dalian, China, 116024

Titanium oxide nanotubes were successfully grown from a titanium plate by direct anodic oxidation with 0.2 wt % hydrofluoric acid being the supporting electrolyte. These nanotubes are of uniform size and are well-aligned into high-density arrays. They look like honeywell with the structure similar to that of porous alumina obtained by the same technique. TiO_2 anatase phase was identified by X-ray diffraction. Significant blue-shift in the spectrum of UV−vis absorption was observed. The mechanism of the novel, simple, and direct growth of the nanotubes was postulated. To investigate their potentials in environmental applications, degradation of pentachlorophenol (PCP) in aqueous solution was carried out using photoelectrocatalytic (PEC) processes, comparing with electrochemical process (EP) and photocatalytic (PC). A significant photoelectrochemical synergetic effect was observed. The kinetic constant of PEC degradation of PCP using TiO_2 nanotubes electrode was 86.5% higher than that using TiO_2 film electrode. In degrading PCP, 70% of TOC was removed using the TiO_2 nanotubes electrode against 50% removed using TiO_2 film electrode formed by sol−gel method in 4 h under similar conditions.

Introduction

Since the first photoelectrocatalytic oxidation study for degrading 4-chlorophenol in aqueous solutions was carried out by Vindogopal et al. (*1*), many research reports for organic pollutants by photoelectrocatalytic technology, such as chlorophenols, dyes, detergent, and organic acids under UV light irradiation (*1*−*5*), were conducted by other researchers. In these studies, photoanodes were TiO_2 film electrodes prepared by coating particle TiO_2 on conducting substrates. Generally speaking, because of its relatively low specific surface area, photocatalytic activity of bulk TiO_2 in these TiO_2 film electrodes needed to improve.

To improve the photocatalytic activity of TiO_2, TiO_2 was modified with doping metal ion, depositing heavy metal, decreasing the size of TiO_2 particle, and so forth. In recent years, because of the large surface area, TiO_2-based nanotubes began to attract wide attention because of their potentials in many areas such as highly efficient photocatalysis (*6*) and photovoltaic cells (*7*, *8*). Titania nanotubes of different geometrical shapes and microstructures in powder forms have been fabricated using techniques such as sol−gel synthesis (*9*−*11*), freeze-drying (*12*), electrodeposition (*13*−*14*), sonochemical deposition (*15*), and chemical treatments of fine titania particles (*16*−*19*). Many of these methods are complicated with the use of templates or chemical processes. Moreover, the titania nanotubes obtained by this way are not supported and thus cannot be used as working electrodes in either electrooxidation or photoelectrocatalytic degradation of pollutants.

Anodic oxidation on aluminum substrate produces porous alumina (*20*). Pu et al. (*21*) prepared individual alumina nanotube on a pure aluminum sheet by anodic oxidation. Such a technique has been proven to be effective for the growth of titania naotubes by Grimes et al. (*22*, *23*). They found that the one-step, templateless method gave large arrays of vertically oriented TiO_2-based nanotubes on the titanium sheet. However, no report has been found so far regarding TiO_2-based nanotubes electrode and its photoelectrocatalytic characteristics. In this study, a TiO_2 electrode as a new type of electrode was produced by forming nanotube-like TiO_2 film on a Ti sheet in an anodization process, and pentachlorophenol (PCP) was used as the target compound under UV irradiation. The objective of this research was to investigate the structural and surface morphology of the TiO_2 nanotube-like electrode and measure its photooxidation efficiency with respect to the degradation of PCP in aqueous solution and photoconversion efficiency using TiO_2 nanotubes electrode. This kind of electrode may find its important roles not only in wastewater purification and photocatalytic waste destruction but also in splitting of water to produce hydrogen and oxygen and selective organic synthesis.

Materials and Methods

Chemicals and Reagents. Pentachlorophenol, HF, and HNO_3 acid were of analytical grade from Shenyang Chemical Company (P.R. China). All compounds were used as received without further purification. Titanium sheet (99.60% purity) was obtained from Beijing Academy of Steel Service, China.

Preparation of TiO_2 Nanotubes Electrode. The titanium sheet was first mechanically polished with different abrasive papers, rinsed in an ultrasonic bath of cold distilled water for 10 min, and then chemically etched by immersing in a mixture of HF and HNO_3 acids for 1 min. The acid mixture ratio of HF:HNO_3:H_2O is 1:4:5 in volume (*24*, *25*). The last step of pretreatment was rinsing with acetone and deionized water. The substrate was then dried in air at room temperature.

The TiO_2 nanotubes electrode was prepared in a cylindrical electrochemical reactor (its radius of the bottom is 30 mm and height is about 70 mm). The electrolyte consisted of 0.2 wt % hydrofluoric acid in water, and a platinum electrode served as the cathode. A previous report on alumina indicated that an anodization voltage of less than 10 V yielded a nanoporous structure and increasing the potential to values greater than 30 V yielded films with a sponge-type appearance (*20*). Hence, a potential of 20 V was used in the present study. All anodization experiments were conducted at room temperature (20 ± 1 °C) with magnetic agitation. In the first few seconds of the anodization, the currents were observed to decrease drastically, and then they approached a stable value. During the anodization experiment, the color of the titanium sheet surface normally changed from purple to blue, yellow, red, and then finally light red.

Characterization of TiO_2 Nanotubes Electrode. The morphology, alignment, and composition of the TiO_2 nanotubes were characterized using scanning electron microscopy (SEM; JSM-5600LV) with an accelerating voltage of 20 kV. An

* Corresponding author tel: +86−411−84706140; fax: +86−411−84706263; e-mail: quanxie@dlut.edu.cn.

10.1021/es048684o CCC: $30.25
Published on Web 04/07/2005

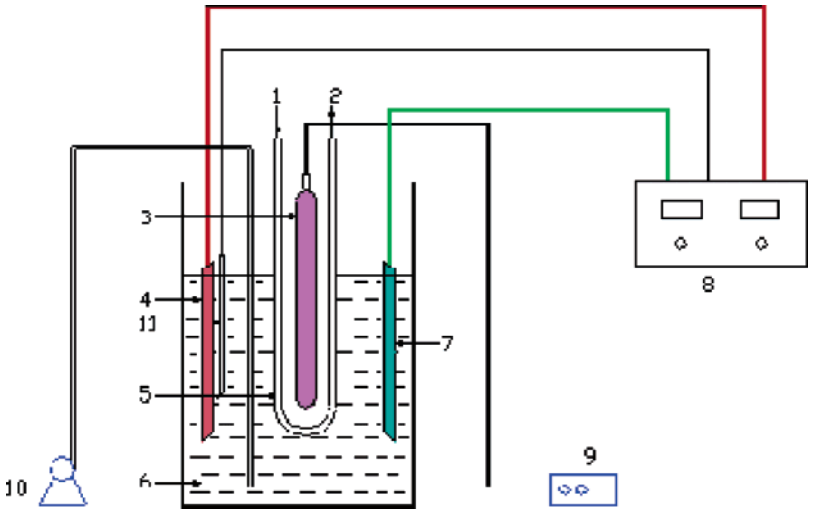

FIGURE 1. The photoelectrocatalytic reactor. (1) Inlet of cooling water; (2) outlet of cooling water; (3) high-pressure mercury lam; (4) working electrode (TiO_2/Ti); (5) quartz sleeve; (6) PCP solutions; (7) counter electrode (stainless steel); (8) potentiostat; (9) manostat; (10) air compressor; (11) reference electrode.

energy-dispersive X-ray spectroscopy (EDX) was equipped with the scanning electron microscope. The crystallinity of the TiO_2 nanotubes was determined by X-ray diffraction (XRD) using a diffractometer with Cu Kα radiation (Model, Shimadzu LabX XRD-6000). The accelerating voltage and the applied current were 40 kV and 30 mA, respectively. Light absorption properties were measured using a UV−vis spectrophotometer (UV-160A) with a wavelength range of 200−800 nm.

Photoelectrocatalytic Experiment. The photoelectrocatalytic degradation was performed in a single photoelectrochemical compartment, as shown in Figure 1. The experiment was performed under the following conditions: under UV irradiation (a 300 W high-pressure mercury lamp from the factory of Shanghai YaMing Light with a maximum wavelength of 365 nm, $I_0 = 0.6$ mW/cm^2), vigorous stirring, 0.5 V (vs SCE) of electric bias, 0.01 mol/L sodium sulfate as electrolyte, and no airflow. The initial concentration of PCP solution was 40 mg/L during the experiment.

Analytical Determination of PCP. The determination of PCP concentrations was performed by HPLC (PU-1580, UV-1575, Jasco Corporation, Japan) with a Kromasil ODS (5 μm, 4.6 mm × 250 mm) reverse-phase column. The mobile phase was 1.0 mL min^{-1} of methanol and water (V:V = 4:1) and was determined at 220 nm.

TOC Analysis. Total organic carbon analyzer (TOC−V_{CPH}, Shimadzu, Japan) was employed for mineralization degree analysis of PCP solutions. Prior to injection into the TOC analyzer, 10−15 mL were collected from the aqueous solutions and were filtrated with 0.45-μm Millipore filter to remove any particles.

Results and Discussion

Morphology of TiO_2 Nanotubes Electrode. Figure 2a is a low-magnification SEM image of the sample showing a large quantity of porous structure. Figure 2b is a high-magnification SEM image of the sample showing much tubular structure. Figure 2c is a tilted plot of TiO_2 nanotubes electrode. These TiO_2 nanotubes are well-aligned and organized into high-density uniform arrays. The tops of the tubes are open, similar to that of porous alumina obtained by anodic oxidation on aluminum. The diameters of these tubes range from 30 to 90 nm and their lengths range from 300 to 500 nm.

XRD Analysis. Figure 3a is an XRD profile of the TiO_2 nanotubes electrode prepared in this work before calcinations. Obviously, an amorphous phase is dominant. After

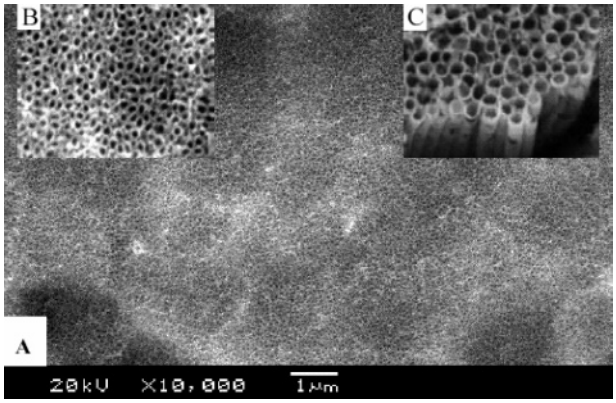

FIGURE 2. SEM images of TiO_2 nanotubes electrode with different magnifications. (A) 10 000× magnification; (B) 50 000× magnification; (C) 80 000× magnification.

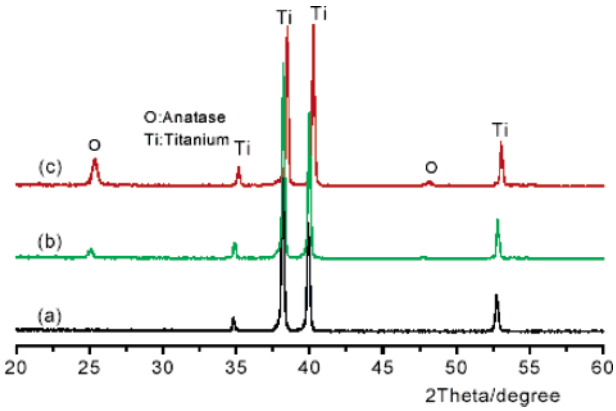

FIGURE 3. X-ray diffraction patterns of TiO_2 electrodes formed by anodic oxidation. (a) Nanotubes without calcinations; (b) nanotubes after calcinations at 450 °C; (c) TiO_2 film.

the TiO_2 nanotubes electrode was calcinated, an anatase phase corresponding to 25.3° appears (Figure 3b). This profile is similar to that of titania nanotubes prepared by sol−gel method (*16*) (Figure 3c). There is no rutile or any other phase in Figure 3b,c.

EDX Analysis. Figure 4 shows selected area energy-dispersive X-ray spectra for two individual nanotubes. The tubes are composed of Ti and O ignoring some undetectable light elements and background signals. Strong Kα and Kβ

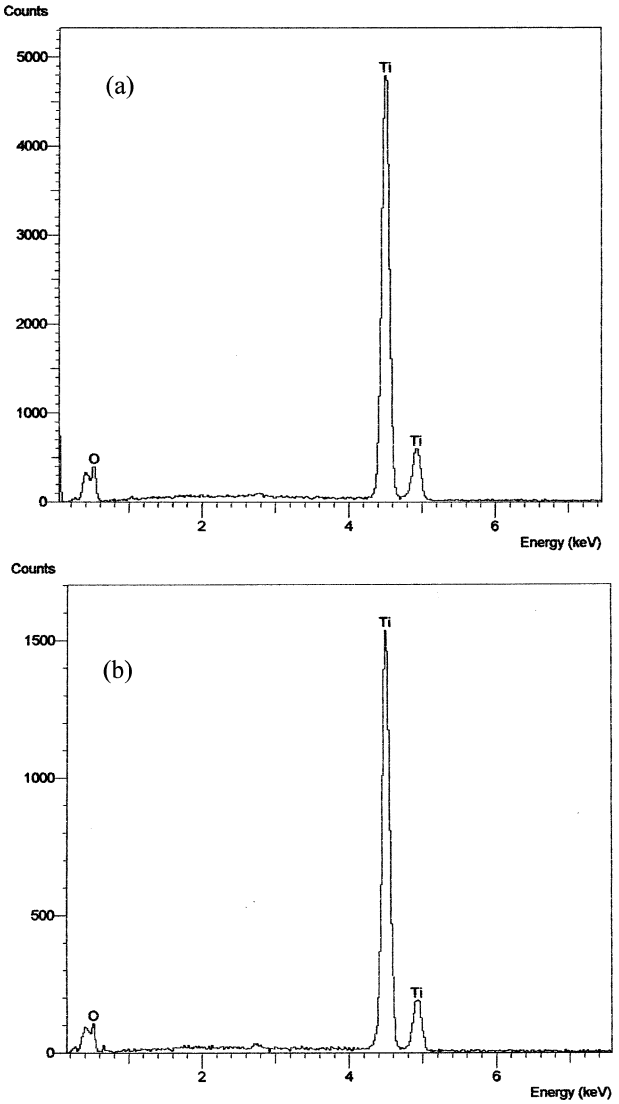

FIGURE 4. Selected area energy-dispersive X-ray spectra of individual microtubes. (a) Nanotubes a and (b) nanotubes b.

signals from Ti were seen at 4.51 and 4.93 keV, respectively. The Lα peak from Ti and the Kα peak from O are so close that they superimpose. Although a quantitative Ti/O ratio analysis has not been performed because of the difficulty of accurately splitting the Kα O peak at 0.523 keV and the Lα Ti peak at 0.452 keV, the approximate Ti/O ratio can be estimated to be 1:2 from the ratio of the heights of the O peak at 0.523 keV and the Ti peak at 4.51 keV. There is no difference in the compositions of the two tubes.

DRS Analysis. The UV−vis adsorption spectrum of the TiO_2 nanotubes and film electrode indicated the maximum adsorption wavelengths are around 260 and 330 nm, respectively (shown in Figure 5). Their band gap absorption edges of the TiO_2 electrode are around 350 nm and 380 nm, respectively, while 387.5 nm is nearly the same as the band gap absorption edge of TiO_2 photocatalyst with band gap energy 3.2 eV. The band gap energy of TiO_2 nanotubes calculated with Kubelka−Munk function (*26*) is about 3.30 eV and that of TiO_2 nanofilm is about 3.22 eV. The significant blue-shift with higher band energy of TiO_2 nanotubes comparing with the TiO_2 film may be owing to the different preparation methods of the two materials, which might cause the differences in the surface state as Takagahara (*27*) explained, although both of them have the same crystalline of anatase (as seen in Figure 3).

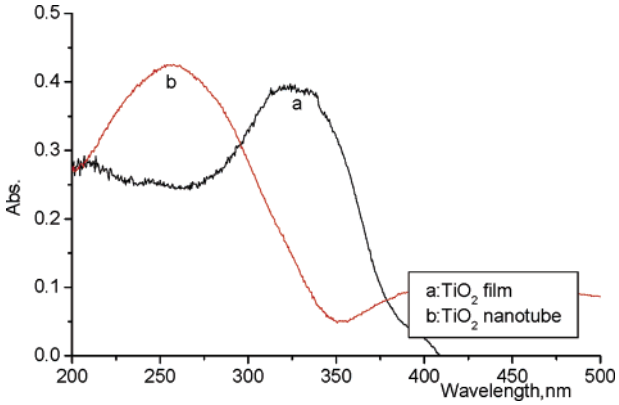

FIGURE 5. UV−vis absorption spectrum of TiO_2 electrodes derived from anodic oxidation on titanium sheet.

Mechanism of the Formation of TiO_2 Nanotubes. One possible reason contributing to the formation of the nanotube structures on titanium during anodization is the competition between dissolution of TiO_2 and growth of TiO_2. During the anodization of titanium sheet, nanotube structures are formed through two processes: field-enhanced oxidation of titanium and field-enhanced oxide dissolution. Inside the pore channel, there are two interfaces: solution/titanium oxide and titanium oxide/titanium. Field-enhanced oxidation occurs at the titanium/titanium oxide interface near the pore bottom when the oxygen-containing ions (O_2^-/OH^-) transport from solution to the oxide layer, along the direction of the pore growth (*22*). At the same time field-enhanced oxide dissolution occurs, titanium ions move from the metal to the solution/titanium oxide interface and dissolve into the solution. The electrical field intensity at the pore bottom is much higher than that at the wall and the solution contains fluorine ions which play an antidote role, so titanium metal will be consumed at a high rate near the bottom of the pore, resulting in continuous growth of the pore depth. In fact, the final thickness of porous titanium oxide film does not increase with the anodizing time (*12*). It may be attributed to the presence of HF in solution, which can etch titanium oxide at a high rate even without an anodizing voltage. If the etching rate of titanium oxide is equal to the growth rate of the titanium oxide either in the wall or at the pore bottom, it will result in a constant thickness of nanotubes (*22*).

Electrochemically Assisted Photocatalytic Degradation of PCP Using Titania Electrode. The electrochemical, direct photolytic (DP), photocatalytic (PC), and photoelectrocatalytic (PEC) processes of PCP in aqueous solutions were performed on TiO_2 nanotubes electrode under given conditions. The electrochemical process of PCP in 4 h was obviously much slower than DP, PC, and PEC processes. The direct photolysis of PCP with UV light alone was proven to be present. The presence of the TiO_2 nanotubes results in the effective photocatalytic decomposition of PCP, and its degradation rate of PCP was rather fast. It may attribute to the photogenerated holes on titania under UV light to decompose PCP quickly. Finally, we checked the photoelectrocatalytic decomposition of PCP, and its degradation rate was the fastest among those processes studied. It is possible that the recombination of photogenerated hole/electron pairs was suppressed by the external electric field, and the longevity of photogenerated carriers remains long. In 4 h, the degradation efficiencies of PCP by electrochemical, direct photocatalytic, photocatalytic, and photoelectrocatalytic process were 8, 57, 70, and 98%, respectively (Figure 6). Therefore, there was an obvious synergetic effect between the electrochemical process and the photocatalytic process.

Comparison of Photoelectrocatalytic Activity. The photoelectrocatalytic degradation of PCP was carried out using

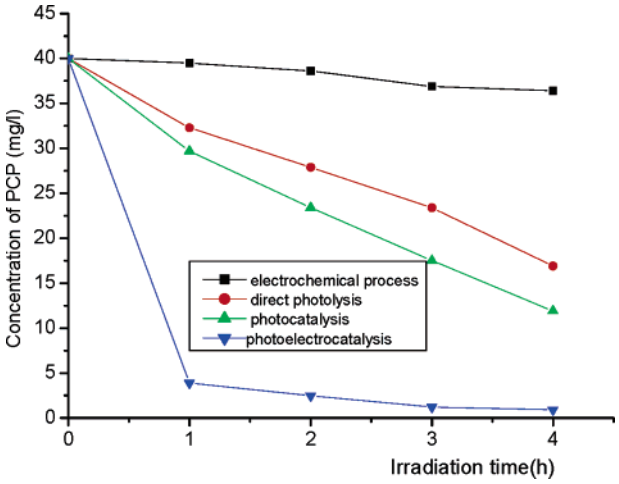

FIGURE 6. The electrochemical process, direct photolysis, photocatalysis, and photoelectrocatalysis of solutions of PCP. TiO_2 nanotubes were used as photocatalysts.

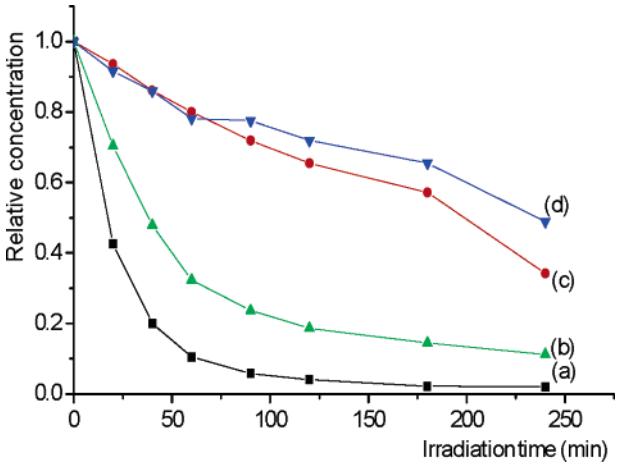

FIGURE 7. The variation of PCP and TOC concentrations by photoelectrocatalytic technology with TiO_2 film and nanotubes electrode. (a) PCP-nanotubes; (b) PCP-film; (c) TOC-nanotubes; (d) TOC-film.

the TiO_2 nanotubes electrode, and the control experiment was also done using titania nanofilm electrode formed by sol−gel method (*28*). Bias potential applied on the TiO_2 film and TiO_2 nanotubes electrode was 0.6 V (vs SCE). The result was presented in Figure 7. It was easily seen from Figure 7 that the TiO_2 nanotubes and film electrode exhibit different photoelectrocatalytic activity. The degradation rate of PCP on TiO_2 nanotubes electrode is faster than that on TiO_2 film electrode. In 4 h, 70% of PCP was mineralized by TiO_2 nanotubes electrode, while about 50% of PCP was mineralized by TiO_2 film electrode. It may be attributed to the difference of band gap energy and specific surface area between the nanotubes and the film. The band gap energy of the TiO_2 nanotubes electrode is higher indicating more powerful photocarriers will be produced under irradiation; in the meantime, TiO_2 nanotubes have larger specific surface area than TiO_2 film and could adsorb more organic matters for degradation.

It is well recognized that the photoelectrocatalytic degradation of organic pollutants accords with pseudo-first-order kinetics (*29*−*31*). In this research, pseudo-first-order kinetics was also confirmed in the electrochemical, photocatalytic, and photoelectrocatalytic process by the linear transforms $\ln(PCP_0/PCP_t) = F(t) = Kt$ (K is kinetic constant). The kinetics constants and regression coefficients of PCP photoelectrocatalysis by TiO_2 nanotubes electrode and TiO_2 film electrode were shown in Table 1. Table 1 indicated that the kinetic constant of PCP oxidation on TiO_2 nanotubes electrode (0.0319 min^{-1}) was 86.5% higher than that on TiO_2 film electrode (0.0171 min^{-1}). It showed that the photocatalytic activity of TiO_2 nanotubes electrode was higher than that of TiO_2 film electrode.

TABLE 1. The Kinetics Constants and Regression Coefficients of PCP Photoelectrocatalysis by TiO_2 Nanotubes Electrode and TiO_2 Film Electrode

electrode	kinetic constant (min^{-1})	R^2
TiO_2 nanotubes	0.0319	0.9254
TiO_2 film	0.0171	0.9826

Photoconversion Efficiency. The photoconversion efficiency E_{eff} of light energy to chemical energy in the presence of an external applied potential E_{app} can be expressed as (*21*)

$$\% E_{eff}(\text{photo}) = j_0 \times (E_{rev}^{\ 0} - |E_{app}|) \times 100\%/I_0 \quad (1)$$

where j_0 is the photocurrent density, $E_{rev}^{\ 0}$ is the standard state-reversible potential (which is 1.23 V for the water-splitting reaction), I_0 is the intensity (power density) of the incident light, and $|E_{app}|$ is the absolute of the applied potential E_{app}.

Figure 8 shows the photoconversion efficiency $\%E_{eff}$ of titania nanotubes and TiO_2 nanofilm in this study. The maximum photoconversion efficiency $\%E_{eff}$ of 12.3% was observed at a minimal applied potential of 0.1 V (shown in Figure 8) when $\%E_{eff}$ was calculated using eq 1. However, under similar conditions of illumination, a maximum $\%E_{eff}$ of 8.17% was observed at a higher applied potential of 0.2 V for the reference TiO_2 nanofilm sample (Figure 8). To have an overview of the photoconversion efficiency $\%E_{eff}$ level in present research, the works reported by Khan et al. (*32*) and Fujishima et al. (*33*) were also presented in Figure 8. The best sample studied by Fujishima et al. generated a maximum photoconversion efficiency of 0.62% at applied potential 0.5 V (vs SCE) (Figure 8) with the existence of Fe^{3+}, and the maximum photoconversion efficiency of a chemically modified titania film reported by Khan et al. was 8.35% at applied potential 0.3 V (vs SCE) without any electrolyte. Although the photoconversion efficiencies of these works were not comparable directly to ours because these experiments were carried out under different conditions, the higher photoconversion efficiency of the present work exhibited the advantage of TiO_2 nanotubes electrode over the TiO_2 nanofilm, which may attributed to its higher band energy and

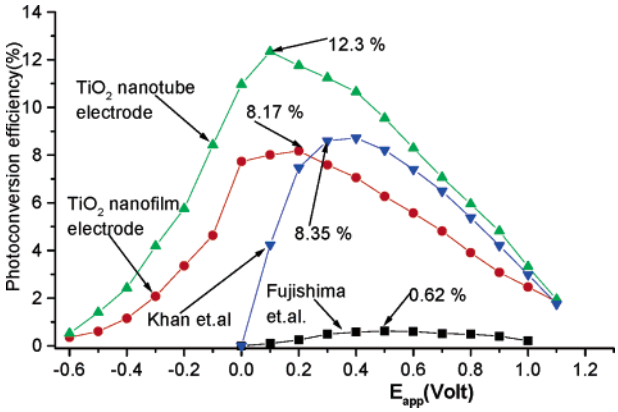

FIGURE 8. Photoconversion efficiency as a function of applied potential. Calculation is shown for study of TiO_2 nanotubes and TiO_2 nanofilm electrode (this study), Khan et al. (*32*), and Fujishima et al. (*33*).

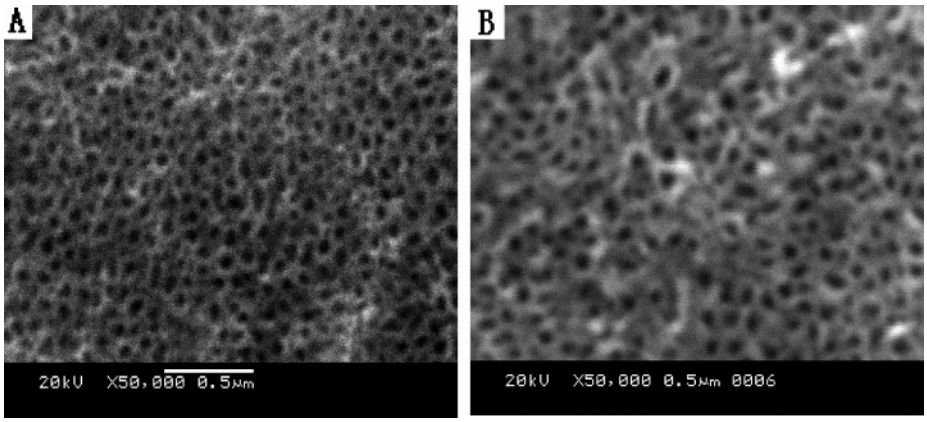

FIGURE 9. The SEM images of TiO_2 nanotubes (A) before experiment and (B) after 10 repeated experiments.

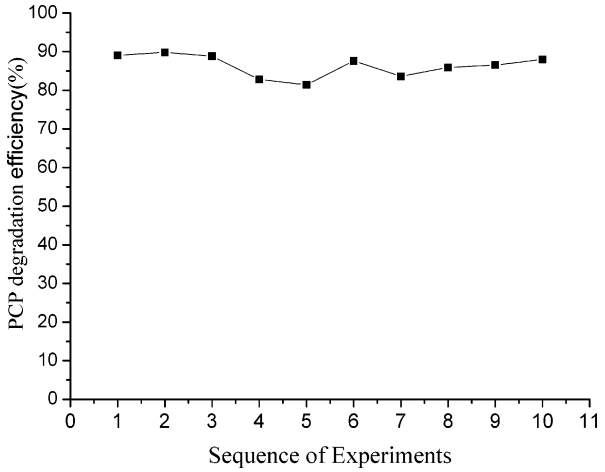

FIGURE 10. PCP photoelectrocatalytic degradation efficiencies of 10 repeated experiments with the TiO_2 nanotubes electrode (experiment condition: 20 mg/L initial concentration of PCP, 0.01 mol/lNa_2SO_4, 2-h irradiation time, light intensity = 0.7 mW/cm^2).

larger specific surface area than the corresponding TiO_2 nanofilm. In addition, the high efficiency of TiO_2 nanotubes may have stemmed from the fact that the nanotubes electrode was prepared at relatively low temperature (<500 °C), and its quality and photoresponse kept well.

Stability of TiO_2 Nanotubes Electrode. To examine the stability of the TiO_2 nanotubes electrode, the photoelectrocatalytic degradation ability of the electrode was investigated 10 times by repeating photoelectrocatalysis experiments of PCP. The TiO_2 nanotubes electrode was cleaned with ultrasonication after each experiment, and then the SEM imagine of the nanotubes was taken. TiO_2 nanotubes could still be seen after being used 10 times but showed a sign of dissolution (Figure 9). However, the results of the 10 repeated experiments for photoelectrocatalytic degradation of PCP in 2 h showed that the degradation efficiencies were rather stable with the RSD being 3.3% (Figure 10).

Generally speaking, the photoconversion ability of titania after modification such as sensitization was improved. For example, $\%E_{eff}$ value of TiO_2 sensitized by 2-[4-bis(methyl)-aminostyryl] benzothiazolium propylsulfonate (BTS) (*34*) was 20.8%, which was higher than the value of 18.3% reported by Licht et al. (*35*), in which AlGaAs/Si RuO_2/Pt was used as an anode. If TiO_2 nanotubes in this study are modified by sensitizing with an appropriate dye such as 2-[4-bis(methyl)-aminostyryl] benzothiazolium propylsulfonate (BTS) or doping a dopant such as C or N, its photoconversion efficiency will be apparently improved. Such an improvement of photoconversion efficiency has important significance in exploring a new efficient photoelectrochemical cell to solve the energy problem.

In a summary, photoconversion ability of titania by modification was greatly improved, yet, as to the titania without any modification, the photoconversion ability of titania nanotubes in this study was rather good.

Acknowledgments

This work was supported jointly by the National Nature Science Foundation P.R. China (project No.20337020) and the Natural Science Foundation of Liaoning Province, China (project No. 20022142).

Literature Cited

(1) Vinodgopal, K.; Hotechandani, S.; Kamat, P. V. Electrochemically assisted photocatalysis. TiO_2 Particulate film electrodes for photocatalytic degradation of 4-chlorophenol. *J. Phys. Chem.* **1993**, *97*, 9040−9044.

(2) Li, X. Z.; Liu, H. L.; Yue, P. T.; Sun, Y. P. Photoelectrocatalytic oxidation of rose bengal in aqueous solution using a Ti/TiO_2 mesh electrode. *Environ. Sci. Technol.* **2000**, *34*, 4401−4405.

(3) Hidaka, H.; Ajisaka, K.; Horikoshi, S.; Oyama, T.; Takeuchi, K.; Zhao, J.; Serpone, N. Comparative assessment of the efficiency of TiO_2/OTE thin film electrodes fabricated by three deposition methods: Photoelectrochemical degradation of the DBS anionic surfactant. *J. Photochem. Photobiol., A: Chem.* **2001**, *138*,185−192.

(4) Vinodgopal, K.; Bedja, I.; Kamat P. V. Nanostructured semiconductor films for photocatalysis. Photoelectrochemical behavior of SnO_2/TiO_2 composite systems and its role in photocatalytic degradation of a textile azo dye. *Chem. Mater.* **1996**, *8*, 2180−2187.

(5) Hidaka, H.; Shimura, T.; Ajisaka, K.; Horikoshi, S.; Zhao, J.; Serpone, N. Photoelectrochemical decomposition of amino acids on TiO_2/OTE particulate film electrode. *J. Photochem. Photobiol., A: Chem.* **1997**, *109*, 165−170.

(6) Adachi, M.; Murata, Y.; Yoshikawa, S. Formation of titania nanotubes with high photo-catalytic activity. *Chem. Lett.* **2000**, *8*, 942−943.

(7) Uchida, S.; Chiba, R.; Tomiha, M.; Masaki, N.; Shirai, M. Application of titania nanotubes to a dye-sensitized solar cell. *Electrochemistry* **2002**, *70*, 418−420.

(8) Adachi, M.; Okada, I.; Ngamsinlapasathian, S.; Murata, Y.; Yoshikawa, S. Dye-sensitized solar cells using semiconductor thin film composed of titania nanotubes.*Electrochemistry* **2002**, *70*, 449−452.

(9) Caruso, R. A.; Schattka, J. H.; Greiner, A. Titanium dioxide tubes from sol-gel coating of electrospun polymer fibers. *Adv. Mater.* **2001**, *13*, 1577−1579.

(10) Hoyer, P. Formation of a titanium dioxide nanotube array. *Langmuir* **1996**, *12*, 1411−1413.

(11) Kasuga, T.; Hiramatsu, M.; Hoson, A.; Sekino, T.; Niihara, K. Formation of titanium oxide nanotube. *Langmuir* **1998**, *14*, 3160−3162.

(12) Ma, D. L.; Schadler, L. S.; Siegel, R. W.; Hong, Jung-Il. Preparation and structure investigation of nanoparticle-assembled titanium dioxide microtubes. *Appl. Phys. Lett.* **2003**, *83*, 1839−1841.

(13) Zhang, Q.; Gao, L.; Sun, J.; Zheng, S. Preparation of long TiO_2 nanotubes from ultrafine rutile nanocrystals. *Hem. Lett*. **2002**, *2*, 226−228.
(14) Adachi, M.; Murata, Y.; Harada, M.; Yoshikawa, S. Formation of titania nanotubes with high photo-catalytic activity. *Chem. Lett*. **2000**, *8*, 942−946.
(15) Zhu, Y.; Li, H.; Koltypin, Y.; Hacohen, Y. R.; Gedanken, A. Sonochemical synthesis of titania whiskers and nanotubes. *Chem. Commun*. **2001**, *24*, 2616−267.
(16) Imai, H.; Takei, Y.; Shimizu, K.; Matsuda, M.; Hirashima, H. Direct preparation of anatase TiO_2 nanotubes in porous alumina membranes *J. Mater. Chem*. **1999**, *9*, 2971−2973.
(17) Kasuga, T.; Hiramatsu, M.; Hoson A.; Sekino, T.; Niihara, K. Titania nanotubes prepared by chemical processing. *Adv. Mater*. **1999**, *11*, 1307−1311.
(18) Du, G. H.; Chen, Q.; Che, R. C.; Yuan, Z. Y.; Peng, L. M. Preparation and structure analysis of titanium oxide nanotubes. *Appl. Phys. Lett*. **2001**, *79*, 3702−3705.
(19) Michailowski, A.; AlMawlawi, D.; Cheng, G. S.; Moskovits, M. Highly regular anatase nanotubule arrays fabricated in porous anodic templates. *Chem. Phys. Lett*. **2001**, *1*, 49.
(20) Zwilling, V.; Darque-Ceretti, E.; Boutry-Forveille, A.; David, D.; Perrin, M. Y.; Aucouturier, M. Structure and physicochemistry of anodic oxide films on titanium and TA6V alloy. *Surf. Interface Anal*. **1999**, *27*, 629−637.
(21) Pu, L.; Bao, X. M.; Zou, J. P.; Feng. D. Individual alumina nanotubes *Angew. Chem., Int. Ed*. **2001**, *40*, 1490−1493.
(22) Gong, D.; Grimes, C. A.; Varghese, O. K.; Hu, W.; Singh, R. S.; Chen, Z.; Dickey, E. C. Titanium oxide nanotube arrays prepared by anodic oxidation. *J. Mater. Res*. **2001**, *16*, 3331−3334.
(23) Varghese, O. K.; Gong, D.; Paulose, M.; Grimes, C. A.; Dickey, E. C. Crystallization and high-temperature structural stability of titanium oxide nanotube arrays. *J. Mater. Res*. **2003**, *18*, 156−165.
(24) Palombari, R.; Ranchella, M.; Rol, C. Oxidative photoelectrochemical technology with Ti/TiO_2 anodes. *Sol Energy Mater. Sol Cells* **2002**, *71*, 359−368.
(25) Fabiana, Y.; Oliva, L. B.; Avalle, E. S. Photoelectrochemical characterization of nanocrystalline TiO_2 films on titanium substrates. *J. Photochem. Photobiol., A: Chem*. **2002**, *146*, 175−188.
(26) Sene, J. J.; Zeltner, W. A.; Anderson, M. A. Fundamental photoelectrocatalytic and electrophoretic mobility studies of TIO_2 and V-Doped TiO_2 thin-film electrode materials. *J. Phys. Chem. B* **2003**, *107*, 1597−1603.
(27) Takagahara, T. Takeda, K. Theory of the quantum confinement effect on excitons in quantum dots of indirect-gap materials. *Phys. Rev. B* **1992**, *46*, 15578−15581.
(28) Yang, S. G.; Quan, X.; Li, X. Y. Preparation,characterization and photoelectrocatalytic properties of nanocrystalline Fe_2O_3/TiO_2, ZnO/TiO_2, and $Fe_2O_3/ZnO/TiO_2$ composite film electrodes towards pentachlorophenol degradation. *Phys. Chem. Chem. Phys*. **2004**, *6*, 659−654.
(29) An, T. C.; Zhu, X. H.; Xiong, Y. Feasibility study of photoelectrochemical degradation of methylene blue with three-dimensional electrode-photocatalytic reactor. *Chemosphere* **2002**, *46*, 897−903.
(30) An, T. C.; Xiong, Y.; Li, G. Y.; Zha, C. H.; Zhu, X. H. Synergetic effect in degradation of formic acid using a new photoelectrochemical reactor. *J. Photochem. Photobiol., A: Chem*. **2002**, *152*, 155−165.
(31) Li, X. Z.; Li, F. B.; Fan, C. M.; Sun, Y. P. Photoelectrocatalytic degradation of humic acid in aqueous solution using a Ti/TiO_2 mesh photoelectrode. *Water Res*. **2002**, *36*, 2215−2224.
(32) Khan, S. U. M.; Al-Shahry, M.; lngler W. B., Jr. Efficient photochemical water splitting by a chemically modified n-TiO_2. *Science* **2002**, *297*, 2243−2245.
(33) Fujishima, A.; Honda K. Electrochemical photolysis of water at a semiconductor electrode. *Nature* **1972**, *238*, 37−38.
(34) Wang, Z. S.; Li, F. Y.; Huang, C. H.; Highly efficient sensitization of nanocrystalline TiO_2 films with styryl benzothiazolium propylsulfonate. *Chem. Commun*. **2000**, *20*, 2063−2064.
(35) Licht, S.; Wang, B.; Mukerji, Soga.; Umeno M., Tributsch. Over 18% solar energy conversion to generation of hydrogen fuel; theory and experiment for efficient solar water splitting. *Int. J. Hydrogen Energy* **2001**, *26*, 653−659.

Received for review August 22, 2004. Revised manuscript received December 28, 2004. Accepted February 10, 2005.

ES048684O